Caving 2026 – A van As, D Cumming-Potvin & J Wesseloo (eds)

doi:10.36487/ACG_repo/2645_87

Velocity model uncertainty in block cave microseismic monitoring: a case for distributed acoustic sensing

Jon Furlong [a,*], **Zara Anderson** [a]

[a] *Sintela Canada Inc, Canada*

Abstract

For microseismic monitoring in mines, velocity model error typically accounts for the largest source of uncertainty in microseismic event location, yet it is routinely underestimated. This paper presents a synthetic modelling study comparing the location performance of distributed acoustic sensing (DAS) to conventional geophone arrays under increasing velocity model perturbation. Using a synthetic 3D velocity model representative of an operating block cave, we demonstrate that the spatial density achievable with DAS provides measurable robustness to velocity model error that sparse geophone arrays cannot match. Array bias, 1-component versus 3-component monitoring, limitations of synthetic-only validation, and the distinction between random and structured velocity perturbations are discussed.

Keywords: *distributed acoustic sensing, DAS, block caving, microseismic monitoring, velocity model, fibre-optic sensing*

1 Introduction

Microseismic monitoring is a foundational element of geotechnical risk management in caving. Cave propagation requires accurate seismic event detection and location for critical decisions like tracking cave shape, designing and scheduling re-entry protocols and ensuring the safety of underground operations (Mendecki et al. 1999).

Yet the industry faces an uncomfortable reality: velocity model error is the single largest source of uncertainty in microseismic event location and is routinely underestimated or disregarded (Morkel et al. 2022). Block caves exist in complex, heterogeneous stress and geological environments that cannot be adequately described by simple velocity models. Constructing accurate velocity models ahead of a caving operation requires detailed modelling and dense spatial sampling of the rock mass. Since quantifying velocity model error is challenging, it is common to assume the error is small. The assumption persists not because it is well supported, but because honestly incorporating an unknown velocity uncertainty into robust processing workflows causes event locations to arbitrarily scatter, source parameters to shift and general confidence metrics to degrade beyond useful limits. The result is a monitoring paradigm built on simplifying assumptions that is widely understood to be inadequate yet accepted as the alternative (acknowledging the true uncertainty) undermines confidence in the output (Tornman & Martinsson 2020).

This paper argues that distributed acoustic sensing (DAS) offers a practical means to address velocity model error not through improved processing (as others have attempted) but by oversampling events spatially at the point of acquisition. By converting an entire length of fibre-optic cable (typically a borehole in mining environments) into thousands of continuously sampled sensing points, DAS provides spatial density that is unavailable to conventional geophone arrays. Rather than attempting to eliminate velocity model uncertainty after the data are collected, dense spatial sampling generates enough independent ray paths through the rock mass that the location solution becomes inherently more robust to model error. This paper is not advocating for replacing geophones (with known advantages) with DAS, but acts as an argument to

* Corresponding author. Email address: jon.furlong@sintela.com

address pitfalls in current seismic monitoring workflows, and a practical look at how dense spatial sampling can help.

2 Background

Conventional microseismic arrays in block caves are typically designed around available mine infrastructure, which is designed for production, not instrumentation (e.g. sensors in the ramp, the drifts, and at the production level). In rare cases, significantly more deliberate instrumentation programs have been deployed (Mercier et al. 2019). Moreover, borehole geophones that extend beyond the mine infrastructure for monitoring are often limited to practical constraints (e.g. 4–6 triaxial sensors per hole, and limited deployment length). The result is that block caves can often remain chronically under-sampled for the velocity structures they are attempting to monitor. The problem worsens with depth: surface stations that once augmented underground arrays become increasingly distant from the sources being monitored, and the mine becomes entirely dependent on its underground infrastructure for spatial coverage (Nordström et al. 2020). This limitation affects both detectability and location accuracy. A single sensor can detect an event, but locating it typically requires 4 or more spatially distributed sensors. This is a known limitation in node-based systems.

DAS is a fibre-optic measurement technique in which backscattered laser light is analysed to measure strain rate at every point along a standard optical fibre, with each section of fibre acting as an independent sensing channel (Rashid et al. 2025). The key property for this study is spatial density: fibre-optic cable costs USD 1–3 per metre and fits in small-diameter boreholes, so a single DAS interrogator monitoring 10–20 km of fibre can instrument the same boreholes as a geophone array but with channels at metre spacing rather than 30–50 m spacing (Lellouch et al. 2020; Furlong & Anderson 2022). This density is what enables dense ray path sampling within the velocity space. Dense ray path sampling is the prerequisite for both robust event locations and for ongoing work in seismic velocity tomography.

3 Methodology

3.1 Model geometry and sensor configuration

The synthetic model represents a block cave footprint including the extraction level, undercut horizon and an upward-propagating cave volume. Four boreholes are positioned approximately evenly around the monitored volume, following standard microseismic array design principles. The geometry was not optimised for a favourable result. It is a loose representation of a mine site one of the authors recently visited, complete with drilled exploration boreholes. This reflects a realistic potential deployment, showing the kind of borehole layout a mine would use.

Both monitoring systems are modelled using the same 4 boreholes to isolate sensor density as the variable under test. The DAS configuration places channels at 5 m spacing along each fibre. This is practical spacing that balances spatial resolution against data volume, as finer spacing (1 m or less) yields diminishing returns for mine seismicity applications. The geophone configuration places up to 4 triaxial sensors per borehole, evenly spaced along the hole length at intervals of 400 m depending on hole depth. This is consistent with typical practice in operating block cave mines (Figure 1).

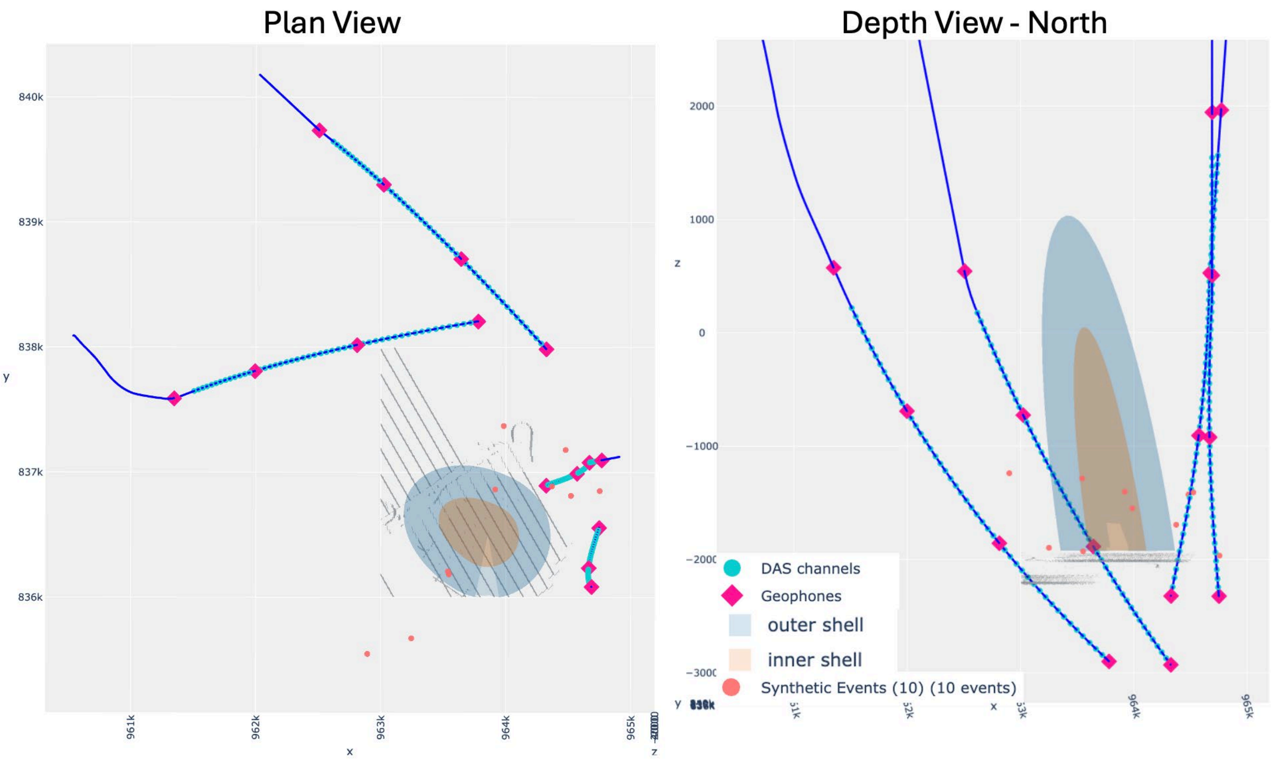

(a) (b)

Figure 1 Illustration of site layout for modelling. (a) Plan view; (b) Depth view. Boreholes are drawn in blue, distributed acoustic sensing (DAS) channels are in teal, geophones in pink, synthetic events as orange dots, inner and outer shell anomalies are plotted as semi-ellipsoids.

3.2 Velocity model

The velocity model is a mildly heterogeneous 3D grid of 100 × 100 × 100 nodes (one million cells), spanning a model space of ~1,800 × 1,800 × 2,300 m (6,000 × 6,000 × 7,500 ft) with cell dimensions of approximately ~18 m (60 ft) horizontally and ~23 m (76 ft) vertically. Host rock P-wave velocity is ~6,000 m/s (19,685 ft/s), representative of competent rock at depth. The cave zone is represented as 2 concentric hemi-ellipsoidal shells with a shared centre and orientation, dipping steeply at 80° from horizontal with an azimuth of 300°. The outer shell represents the fractured rock zone surrounding the cave, with a P-wave velocity of ~5,182 m/s (17,000 ft/s), a 14% reduction from the background host material. The inner shell represents highly fractured and mobilised material, with a P-wave velocity of 3,658 m/s (12,000 ft/s), a ~40% reduction. We do not model any pure voids in the cave as they are rare and will introduce numerical instabilities in modelling. The S-wave velocities are derived from the P-wave model using a Vp/Vs ratio of 1.7.

The velocity contrasts, while somewhat arbitrarily contrived in this simple model, represent possible real-world ray paths bending through a caving zone without being too 'extreme' for visualisation purposes.

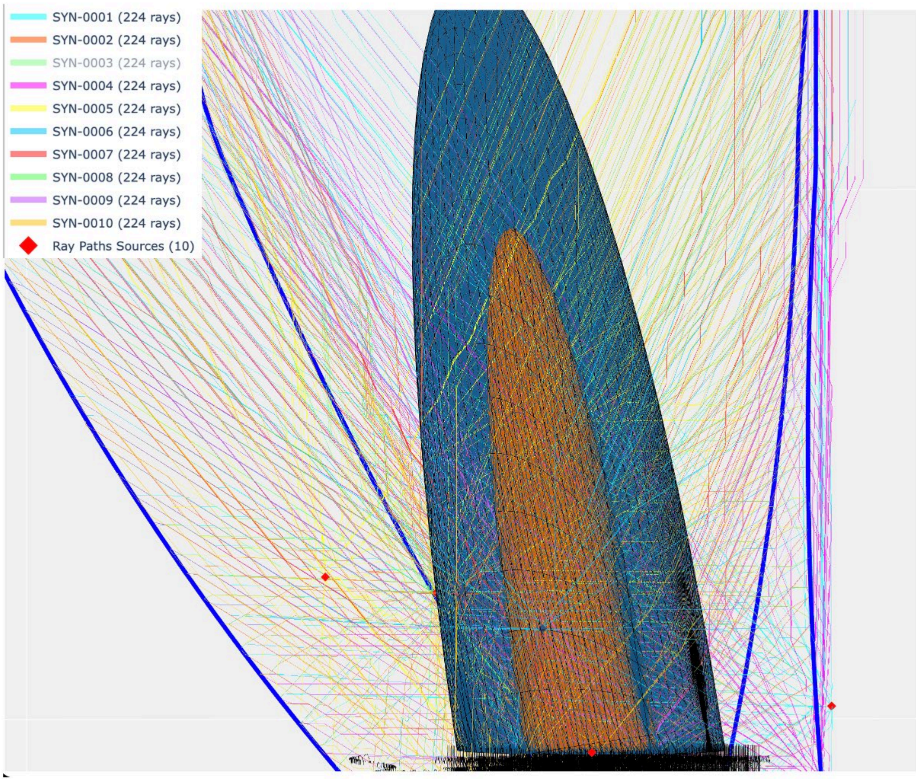

Figure 2 3D view of a mine with approximate ray paths modelled through velocity anomaly

3.3 Synthetic waveform generation and event location

Synthetic seismic events are generated using a custom Python toolchain (synthms) built on ttcrpy for 3D eikonal travel time computation and ray path tracing, with ObsPy for waveform filtering and export, and SciPy/NumPy for signal processing. Travel times are computed for both P and S phases for each source-receiver pair through the heterogeneous velocity model.

Event locations are computed using QuakeMigrate (Winder et al. 2022; Hudson et al. 2025), a migration-based location algorithm that stacks waveform energy across the receiver array to identify the most likely source position. The migration approach differs from classical pick-based location methods in that it does not require explicit phase arrival picks. Instead, it evaluates the coherence of the waveform signal across all receivers for candidate source locations throughout the model volume. QuakeMigrate natively supports homogeneous and 1D layered velocity models. For this study, it has been adapted to accept 3D heterogeneous velocity models.

3.4 Detection and location criteria

All events (geophones and DAS) are located using QuakeMigrate, a migration-based detector and locator that continuously stacks waveform energy across all channels without requiring a minimum number of station detections, a minimum signal-to-noise ratio or a minimum pick quality. QuakeMigrate computes a continuous onset (characteristic) function per channel and pre-computes P and S travel time lookup tables from every node of a 3D grid to every receiver. Then, for each candidate origin time and node, you back-shift and stack the onset functions. Real sources produce constructive coherence (a peak in the 4D coalescence volume), while noise stacks incoherently. Detection and location become the 'same' operation: you detect by locating every event for which waveform data exist, with the coalescence value (COA) serving as the post hoc quality indicator. This approach is well suited to comparing the 2 array configurations because it makes no assumptions about detection geometry; both systems are evaluated on equal terms by the same algorithm (Porras et al. 2024).

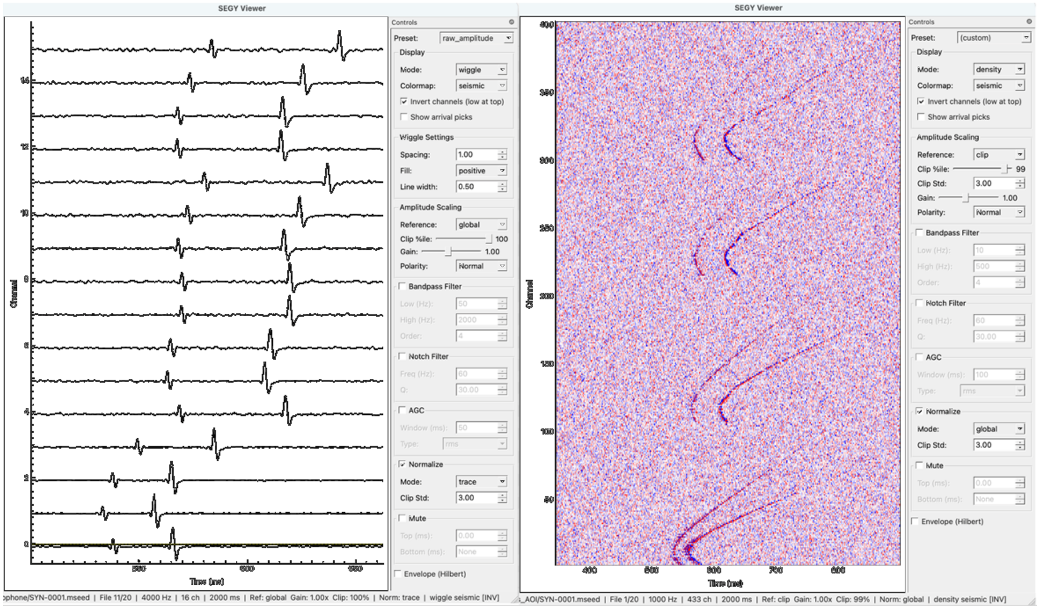

(a) (b)

Figure 3 Synthetic DAS arrivals for Event 1 based on velocity model anomaly. (a) Event detected on geophone; (b) Event detected by DAS

For the geophone configuration, sensor separations of tens to hundreds of metres ensure that detections at different stations represent independent ray paths through the velocity model. For DAS, spatial proximity alone is insufficient to guarantee independence; adjacent channels (25 m spacing) share similar ray paths, coupling conditions, and noise characteristics.

Weak events are expected to produce low COA values and degraded location accuracy regardless of array configuration. This degradation is a result of interest in its own right, not a modelling failure.

4 Results

The generated synthetic events are relocated with the same modelled velocity model in Figure 4. The event location metadata are included in Table 1.

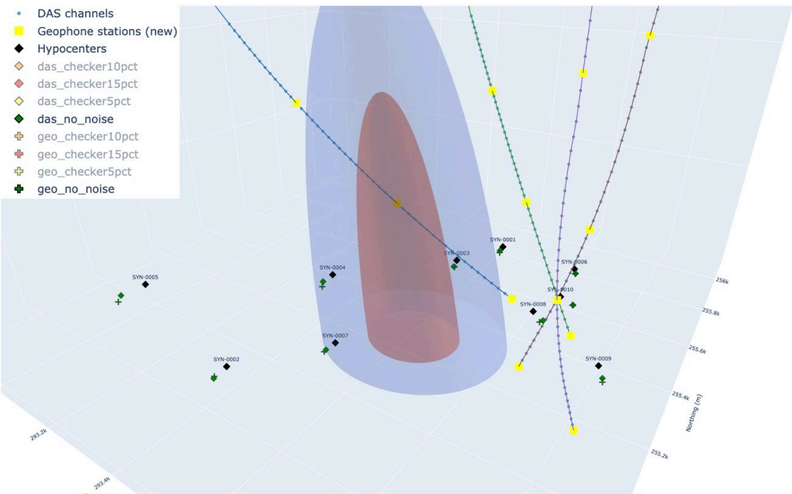

Figure 4 Events locations shown for geophones (green crosses) and DAS (green squares) based on passing synthetics generated on known source locations (black diamonds) and array geometry. For Mw of −1.0, the locations of the geophones and DAS are comparable, and additional sensor density provides marginal improvements in event location accuracy

Table 1 COA values are dimensionless and unchanged. Δ = DAS improvement over geophone 3D error; positive values indicate DAS located the event closer to truth. DAS improves location by a mean of 9.8 ft over geophone (85.2 ≥ 75.5 ft). DAS is better on 8 of 10 events, but the improvement is modest, ranging from 1.1 ft (SYN-0008) to 29.4 ft (SYN-0004). On 2 events (SYN-0002 and SYN-0010) geophone is better by a small margin. At Mw −1.0, both arrays have sufficient signal-to-noise ratio (SNR) and the location accuracy difference is not dramatic

Event	Geo 3D err (m)	Geo COA	DAS 3D err (m)	DAS COA	Δ (m)
SYN-0001	17.4	16.97	11.9	24.16	+5.5
SYN-0002	25.5	6.62	32.1	7.12	−6.6
SYN-0003	18.6	13.82	16.7	18.70	+1.9
SYN-0004	32.4	11.71	23.4	14.36	+9.0
SYN-0005	48.7	5.14	40.2	6.50	+8.6
SYN-0006	11.2	13.09	10.2	19.43	+1.1
SYN-0007	26.4	8.90	23.6	11.86	+2.8
SYN-0008	24.2	12.53	23.9	18.49	+0.3
SYN-0009	32.4	13.56	24.6	13.42	+7.7
SYN-0010	22.9	12.44	23.5	16.56	−0.5
Mean	**26.0**	**11.48**	**23.0**	**15.06**	**+3.0**
Std dev	10.3	–	8.9	–	–

4.1 Array bias

DAS arrays are inherently susceptible to array bias the tendency for event locations to be pulled toward the densest concentration of detecting sensors. Because DAS channels are closely spaced along a linear fibre path, the location algorithm receives a large number of observations from a narrow spatial corridor. QuakeMigrate, like most location algorithms, takes receiver positions as inputs without explicitly accounting for spatial correlation between adjacent channels. Any array bias is therefore embedded in the result.

This limitation must be clearly understood. When all 4 fibres contribute detections (providing spatial sampling from multiple azimuths around the source), array bias is mitigated by the geometric diversity of the array. However, when a weak event is detected on only 1 or 2 fibres, the location is poorly constrained and will be systematically drawn toward the detecting fibre(s).

This is not unique to DAS. Geophone arrays exhibit equivalent degradation when events are detected on only 1 or 2 widely separated stations (neither system performs well with poor geometry). The difference is that DAS, by its nature as a densely sampled linear array, is more prone to this failure mode when fibre coverage is insufficient.

4.2 Velocity model error sensitivity

The central analysis of this paper tests the hypothesis that the spatial density of DAS provides greater robustness to velocity model error than a conventional geophone array.

The same set of synthetic events is located using the DAS and geophone configurations in the true velocity model. Random velocity perturbations are then applied to the model (each cell's velocity is independently perturbed by a random amount) and the events are relocated under increasing levels of perturbation (Figure 5). Random perturbations were chosen for this study because they are the most intuitive form of velocity model error for the audience to interpret, though it is acknowledged that real velocity model errors tend to be structured rather than random (see Section 5.1). We then measure the extent to which location accuracy degrades as the velocity error increases. The expectation is that because DAS samples more independent ray paths through the rock mass, the DAS locations show lower location error compared to geophones when the velocity model is perturbed. Table 2 outlines the failure of DAS and geophones together, and how they trend. An important aspect to note is the ratio of true location errors (known location less modelled location) to the Gaussian 3D error computed via QuakeMigrate. The ratio indicates whether an estimate of error for an event is reliable.

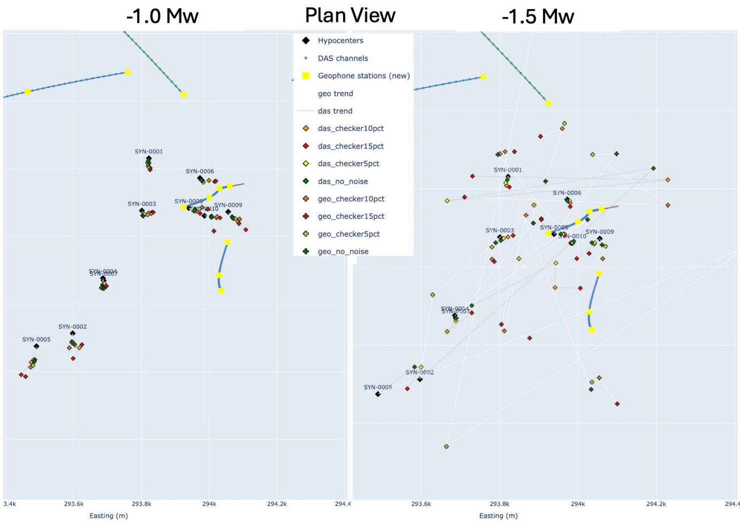

Figure 5 **Application of random velocity model error via ~91 m (300 ft) cubic sections of ±5, 10 and 15% velocity model error. Lines are drawn from events located with no noise, to events with 5, 10 then 15% sequentially. Geophone progression through sequential error is shown in white, DAS is shown in black. While geophone and DAS both show significant susceptibility to random errors being applied to the data, DAS fails slower when compared to geophones**

Table 2 **COA, SNR, channel rates, picks and pick residuals are dimensionless or in seconds and unchanged. The error/uncertainty ratio is the key calibration metric: values <1 indicate the reported uncertainty bounds the true error; values >1 mean the location is confidently wrong**

Metric	Geophone Mw −1.0 (16 stations)	Geophone Mw −1.5 (16 stations)	DAS Mw −1.0 (200 stations)	DAS Mw −1.5 (200 stations)
Events located	10/10	9/10	10/10	10/10
Mean 3D location error (m)	26.0	363.2	23.0	108.4
Std dev 3D error (m)	10.3	325.6	8.9	24.8
Min./max. error (m)	11.2/48.7	18.0/1,040	10.2/40.2	6.3/813.7
Mean depth bias dZ (m)	+12.4	+76.3	+7.6	−14.4
Mean COA	11.48	2.01	15.06	2.06
Channel detection rate	76%	19%	86%	22%
Mean detecting picks/event	24/32	6/32	345/400	86/400
Mean SNR (detecting channel)	46.9	9.8	75.6	5.99
Mean |pick residual| (s)	0.0042	0.0249	0.0037	0.0152
Mean reported uncertainty (m)	100.8	191.7	96.1	226.0
Error/uncertainty ratio	0.26	1.87	0.24	0.39
Events exceeding uncertainty	0/10	6/9	0/10	0/10

5 Discussion

5.1 Limitations of this study

The velocity model error sensitivity test uses random perturbations as a first-order test of robustness. Real velocity model errors in mines are not random (they are structural). Mislocated cave boundaries, misplaced lithological contacts, and systematic bias from sparse data produce correlated errors that affect ray paths in ways that random perturbations do not fully capture. Structured perturbation testing is a natural extension of this work and would provide a more rigorous demonstration of the value of dense spatial sampling under realistic error conditions.

This study is entirely synthetic, and no field validation is presented. However, published field comparisons between DAS and geophones at operating mines are consistent with the results shown here, and similar comparisons are available in other industries (Hey Tow et al. 2023; Dande et al. 2024; Lellouch et al. 2020, 2021; Hudson et al. 2021; Zhang et al. 2023).

5.2 DAS future developments

Array bias remains a genuine concern. When events are detected on only 1 or 2 fibres, locations are poorly constrained and systematically drawn towards the detecting fibre. Multi-borehole geometries mitigate this effect, but single-fibre or limited-fibre deployments must be interpreted with caution.

Moment tensor inversion from DAS data is an active area of academic research with published solutions demonstrating feasibility (Bader et al. 2023), but commercial implementations are not yet available. Until moment tensor products are available in operational processing software, mines requiring routine focal mechanism analysis will continue to depend on triaxial geophone data (Pesicek et al. 2016). Similarly, magnitude estimation from strain rate is advancing rapidly with published DAS versus geophone comparisons showing good agreement, but industry processing tools have not yet fully incorporated strain rate–based magnitude estimation (Lior 2024; Chen 2023).

Some areas of a block cave, active drawpoints, congested production level infrastructure, and areas subject to frequent physical disturbance, may be better served by individual geophones that can be placed quickly. For rapid baseline monitoring or for filling a short-notice gap in coverage, a single geophone deployed within hours remains simpler than any DAS configuration.

6 Conclusion

These results demonstrate that the spatial density achievable with DAS provides a measurable advantage in the specific area where mining seismology is most vulnerable and the velocity model is uncertain. DAS does not replace conventional geophone networks, which remain effective and operationally proven. Rather, the 2 technologies are most effective when deployed together, and for their respective strengths: geophones for 3-component recording, moment tensor analysis and rapid deployment; DAS for spatial density, velocity model robustness and scalable coverage. For block caving operations where the rock mass is heterogeneous, access is constrained, and the consequences of poor event location affect safety-critical decisions, this complementary capability has practical value.

References

Bader, M, Clapp, RG, Nihei, KT & Biondi, B 2023, 'Moment tensor inversion of perforation shots using distributed acoustic sensing', *Geophysics*, vol. 88, no. 3, pp. KS57–KS67.

Chen, X 2023, 'Source parameter analysis using distributed acoustic sensing — an example with the PoroTomo array', *Geophysical Journal International*, vol. 235, no. 3, pp. 2577–2588.

Dande, S, Forbes, E, Butler, T, Graham, K, Hawryluck, C, Hall, A, … Cherubini, A 2024, 'Utilising distributed acoustic sensing for monitoring rock mass stress conditions in underground mining: a case study', *Sensors*, vol. 24, no. 7, p. 2208.

Furlong, J & Anderson, Z 2022, 'Distributed acoustic sensing/distributed strain sensing technology and its applications for block cave progress monitoring, rock mass preconditioning, and imagining', in Y Potvin (ed.), *Caving 2022: Proceedings of the Fifth International Conference on Block and Sublevel Caving*, Australian Centre for Geomechanics, Perth, pp. 991–1006, https://doi.org/10.36487/ACG_repo/2205_68

Hey Tow, K, Pereira, J, Lindblom, M, Fernández-Ruiz, MR, Martins, HF, Rossi, M, Nilsson, S & van den Berg, H 2023, 'Monitoring mining induced seismicity using optical fibre sensors during mine exploitation', *Proceedings of SPIE*, vol. 12643, 1264305.

Hudson, TS, Baird, AF, Kendall, JM, Kufner, SK, Brisbourne, AM, Smith, AM, Butcher, A, Chalari, A & Clarke, A 2021, 'Distributed acoustic sensing (DAS) for natural microseismicity studies: a case study from Antarctica', *Journal of Geophysical Research: Solid Earth*, vol. 126, no. 7, e2020JB021493.

Hudson, TS, Klaasen, S, Fontaine, O, Bacon, CA, Jónsdóttir, K & Fichtner, A 2025, 'Towards a widely applicable earthquake detection algorithm for fibreoptic and hybrid fibreoptic-seismometer networks', *Geophysical Journal International*, vol. 240, no. 1, pp. 1–18.

Lellouch, A, Lindsey, NJ, Ellsworth, WL & Biondi, BL 2020, 'Comparison between distributed acoustic sensing and geophones: downhole microseismic monitoring of the FORGE geothermal experiment', *Seismological Research Letters*, vol. 91, no. 6, pp. 3256–3268.

Lellouch, A, Schultz, R, Lindsey, NJ, Biondi, BL & Ellsworth, WL 2021, 'Low-magnitude seismicity with a downhole distributed acoustic sensing array — examples from the FORGE geothermal experiment', *Journal of Geophysical Research: Solid Earth*, vol. 126, no. 4, e2020JB020462.

Lior, I 2024, 'Accurate magnitude and stress drop using the empirical Green's function method applied to distributed acoustic sensing', *Geophysical Research Letters*, vol. 51, no. 3, e2023GL107475.

Mendecki, AJ, van Aswegen, G & Mountfort, P 1999, 'A guide to routine seismic monitoring in mines', in AJ Jager & JA Ryder (eds), *A Handbook on Rock Engineering Practice for Tabular Hard Rock Mines*, Safety in Mines Research Advisory Committee, pp. 287–309.

Mercier, J-P, van As, A, Carlson, C & Tumur-Ochir, B 2018, 'Microseismic monitoring of the Oyu Tolgoi Hugo North Lift 1', in Y Potvin & J Jakubec (eds), *Caving 2018: Proceedings of the Fourth International Symposium on Block and Sublevel Caving*, Australian Centre for Geomechanics, Perth, pp. 823–834, https://doi.org/10.36487/ACG_rep/1815_65_Mercier

Morkel, IG, Wesseloo, J & Potvin, Y 2022, 'Seismic event location uncertainty in mining with reference to caving', in Y Potvin (ed.), *Caving 2022: Proceedings of the Fifth International Conference on Block and Sublevel Caving*, Australian Centre for Geomechanics, Perth, pp. 445–460, https://doi.org/10.36487/ACG_repo/2205_30

Nordström, E, Dineva, S & Nordlund, E 2020, 'Back analysis of short-term seismic hazard indicators of larger seismic events in deep underground mines (LKAB, Kiirunavaara Mine, Sweden)', *Pure and Applied Geophysics*, vol. 177, no. 2, pp. 763–785.

Pesicek, JD, Ciéslik, K, Lambert, M-A, Carrillo, P & Birkelo, B 2016, 'Dense surface seismic data confirm non-double-couple source mechanisms induced by hydraulic fracturing', *Geophysics*, vol. 81, no. 6, pp. KS207–KS217.

Porras, J, Pecci, D, Bocchini, GM, Gaviano, S, De Solda, M, Tuinstra, K, Lanza, F, Tognarelli, A, Stucchi, E & Grigoli, F 2024, 'A semblance-based microseismic event detector for DAS data', *Seismological Research Letters*, vol. 95, no. 5, pp. 2995–3008.

Rashid, A, Tackie-Otoo, BN, Abdul Latiff, AH, Otchere, DA, Jamaludin, SNF & Asfha, DT 2025, 'Research advances on distributed acoustic sensing technology for seismology', *Journal of Applied Geophysics*, vol. 223, 105601.

Törnman, W & Martinsson, J 2020, 'Reliable automatic processing of seismic events: solving the Swiss cheese problem', in J Wesseloo (ed.), *UMT 2020: Proceedings of the Second International Conference on Underground Mining Technology*, Australian Centre for Geomechanics, Perth, pp. 155–172, https://doi.org/10.36487/ACG_repo/2035_04

Winder, T, Bacon, CA, Smith, JD, Hudson, TS & White, RS 2022, 'QuakeMigrate: a Python package for automatic earthquake detection and location using waveform migration and stacking', *Seismica*, vol. 1, no. 1.

Zhang, Z-D, White, MCA, Bai, T, Qiu, H & Nakata, N 2023, 'Characterizing microearthquakes induced by hydraulic fracturing with hybrid borehole DAS and three-component geophone data', *Geophysics*, vol. 88, no. 3, pp. KS69–KS83.